COMPUTING COHERENT SYNCHROTRON RADIATION FROM LIÉNARD-WIECHERT POTENTIALS

M. Schwarz*, A. Bernhard, M. Brosi, J. Schäfer, A.-S. Müller
Karlsruhe Institute of Technology, Karlsruhe, Germany

Abstract

The linac-based test accelerator FLUTE contains a bunch compressor to create few-fs scale bunches that generate coherent radiation in the THz regime. The form and spectrum of the THz pulse strongly depend on the evolution of the bunch along the bunch compressor, and hence on the paths of the particles. From a given path of a charged particle, one can compute the emitted radiation by means of the Liénard-Wiechert potentials. A problem with this approach is that one needs to solve an implicit equation for the retarded time. Here, we instead compute the retarded time from the particle time and observer position. Furthermore, the Liénard-Wiechert potentials depend on the acceleration, while macro-particle tracking only yields the particle positions and momenta at fixed times. To compute the acceleration, we interpolate the data using twice differentiable functions. We compare the numerical results to the analytical benchmark case of synchrotron radiation. Finally, we compute the coherent radiation emitted by a simulated bunch during compression.

INTRODUCTION

The electric field of a point particle of charge q, moving on a path $\boldsymbol{r}(t)$ is given by the Liénard-Wiechert field [1]. Since we are interested in the emitted radiation, we neglect the Coulomb term, and focus on the radiation term:

$$\boldsymbol{E}_{\mathrm{rad}}(t_{\mathrm{obs}}, \boldsymbol{r}_{\mathrm{obs}}) = \frac{q\, Z_0}{4\pi} \left. \frac{\boldsymbol{n} \times \left[(\boldsymbol{n} - \boldsymbol{\beta}) \times \dot{\boldsymbol{\beta}} \right]}{(1 - \boldsymbol{\beta} \cdot \boldsymbol{n})^3 \, R} \right|_{\mathrm{ret}} . \quad (1)$$

Here, $\boldsymbol{\beta} = \dot{\boldsymbol{r}}/c$ and $\dot{\boldsymbol{\beta}}$ denote the scaled velocity and acceleration of the particle. The observer is located at the spatial position $\boldsymbol{r}_{\mathrm{obs}}$ and receives the field at the time t_{obs}. The unit vector $\boldsymbol{n}$ points from the particle to the observer. Due to the finite speed of light c, a given observer time t_{obs} is related to the retarded time by

$$t_r = t_{\mathrm{obs}} - R(t_r)/c \, , \quad (2)$$

where $R(t_r) = |\boldsymbol{r}_{\mathrm{obs}} - \boldsymbol{r}(t_r)|$ is the distance from the particle to the observer. The field in Eq. (1) have to be evaluated at t_r.

To calculate the field at the observer position and time one needs to know the particle state at the earlier time when the radiation was emitted such that it reaches the observer at $(t_{\mathrm{obs}}, \boldsymbol{r}_{\mathrm{obs}})$. The problem is that Eq. (2) is an implicit equation for $t_r(t_{\mathrm{obs}})$, which is difficult to solve even for simple analytic cases. One solution is to compute the fields in the frequency domain by a Fourier transform. One can then perform a substitution of variables and work directly with t_r. This approach is used on programs such as `SRW` [2] and `spectra` [3]. It works well in the paraxial approximation, but this approximation breaks down for THz frequencies. Another solution is to work in the time domain and solve Eq. (2) by a root-finding algorithm [4]. However, the root-finding needs to work to high precision, since t_r is often in the ns-scale while t_{obs} is in the fs-scale.

In this paper, we work in the time domain, but instead of trying to compute $t_r(t_{\mathrm{obs}})$, we compute the observer time from the particle path $\boldsymbol{r}(t_p)$ as

$$t_{\mathrm{obs}}(t_p) = t_p + R(t_p)/c \, , \quad (3)$$

which is straightforward for a given particle path $\boldsymbol{r}(t_p)$. The time t_p that parametrizes the particle path equals the retarded time. First the r.h.s. of Eq. (1) is evaluated for t_p, yielding $\boldsymbol{E}_{\mathrm{rad}}(t_p, \boldsymbol{r}_{\mathrm{obs}})$. Then we use Eq. (3) to obtain $\boldsymbol{E}_{\mathrm{rad}}(t_{\mathrm{obs}}(t_p), \boldsymbol{r}_{\mathrm{obs}})$. From this point of view, Eq. (3) is just a non-linear rescaling of the time axes.

Given the electric field in the time domain, one can compute the spectrum of the emitted radiation by

$$\left. \frac{\mathrm{d}^2 I}{\mathrm{d}\Omega \, \mathrm{d}\omega} \right|_1 = 2 \sqrt{\frac{\epsilon_0}{\mu_0}} \, |\mathrm{FT}\{R\, \boldsymbol{E}, \omega\}|^2 \, , \quad (4)$$

where FT denotes the Fourier transform. Notice that the Fourier transform has to be done w.r.t. the observer time t_{obs}. The index 1 indicates that it is the spectrum of a single particle. To obtain the spectrum emitted by N particles, one first has to sum the electric fields of the particles and then take the modulus. For analytical results, the sum over particles is replaced by an integration over a charge density [5], which results in

$$\left. \frac{\mathrm{d}^2 I}{\mathrm{d}\Omega \mathrm{d}\omega} \right|_N = \left[N + N^2 F(\omega) \right] \left. \frac{\mathrm{d}^2 I}{\mathrm{d}\Omega \mathrm{d}\omega} \right|_1 . \quad (5)$$

Here, F denotes the form factor, which is the squared modulus of the Fourier-transformed line density. It measures the "degree of coherence" of the radiation at (angular) frequency ω, with 1 meaning fully coherent and 0 meaning incoherent. Notice that the coherent radiation scales with the number of particles squared.

SOLVER ALGORITHM

Typically, tracking codes provide 6D phase space coordinates $(\boldsymbol{r}_j, \boldsymbol{p}_j)$ of the macro-particles at positions s_j or times $t_{p,j}$. While it is straightforward to compute the velocities $\boldsymbol{\beta}_j$ from the momenta $\boldsymbol{p}_j$, the acceleration $\dot{\boldsymbol{\beta}}_j$ is usually not

* Markus.Schwarz@kit.edu

provided but is needed in Eq. (1). The first step is to obtain the acceleration. We create functions $\boldsymbol{r}(t_p)$, $\boldsymbol{\beta}(t_p)$ by interpolation of the data $(t_{p,j}, \boldsymbol{r}_j, \boldsymbol{\beta}_j)$. By interpolating with B-splines it is possible to create C^2 curves that allow for obtaining a continuous acceleration $\dot{\boldsymbol{\beta}}(t_p)$ as well. We can then use the interpolated functions to compute $\boldsymbol{E}_{\mathrm{rad}}(t_p, \boldsymbol{r}_{\mathrm{obs}})$ from Eq. (1). In the final step, we compute $t_{\mathrm{obs}}(t_p)$ by using Eq. (3).

A second advantage of the interpolated functions is that they allow us to compute the electric field at arbitrary times t_p and not just at the discrete $t_{p,j}$. The minimum and maximum values of the $t_{p,j}$ set the range of the continuous variable t_p. We use the python package `Adaptive` [6] to non-uniformly sample the electric field $\boldsymbol{E}_{\mathrm{rad}}(t_p, \boldsymbol{r}_{\mathrm{obs}})$: densely sampled at peaks and sparsely sampled in the tails.

The disadvantage is that this prevents the use of the fast Fourier transform (FFT) to compute spectra. On the other hand, a semi-analytic Fourier transform [7] works for non-uniformly sampled data at arbitrary frequencies. We are typically interested in the frequency range 0.1 THz to 100 THz, which would require 10 000 equally spaced data points for the required 5 fs resolution. This also puts a heavy demand on system memory. With the semi-analytic approach, we require about 100 non-equidistant data points.

To compute the spectrum of N macro-particles we need to sum their electric fields at the same times t_{obs}. However, for the same t_p Eq. (3) yields a different $t_{\mathrm{obs},n}$ for each macro-particle n because their positions are different. First, we define a set of common $t_{p,c}$ at which to evaluate the fields of all particles and compute $(t_{\mathrm{obs},n}(t_{p,c}), \boldsymbol{E}_n)$. Second, we create functions $\boldsymbol{E}_n(t_{\mathrm{obs}})$ by linearly interpolating the data points. Fields are put to 0 outside the interpolation time intervals. We obtain the common times $t_{p,c}$ by adaptively sampling [6] the fields of a few macro-particles. Typically 10 out of 10 000 are sufficient. For the spectrum, we compute the Fourier transform $\mathrm{FT}\{R_n \boldsymbol{E}_n, \omega\}$ for each macro-particle and sum the result before taking the modulus.

Analytic Benchmark

Table 1: Simulation Parameters

Quantity	Value
Energy (γ)	42.4 MeV (83)
Bending radius	2.35 m
Critical frequency f_{crit}	17.4 THz
# macro-particles	10 000
# screen pixels	650
Screen radius	12.5 mm

We benchmark our algorithm against the textbook case of an electron moving on a circle. The parameters are given in Table 1 and correspond to the values of the FLUTE bunch compressor discussed in the next section.

We create mock 'simulated' data by sampling the analytic path $\boldsymbol{r}(t_p)$, $\boldsymbol{\beta}(t_p)$ at 50 equally spaced times between $(-T_{\mathrm{rev}}/50, +T_{\mathrm{rev}}/50) \approx (-985\,\mathrm{ps}, 985\,\mathrm{ps})$. As a first cross-check, we compute the relative deviation between the analytic acceleration and the one from the B-spline interpolation, and find it to be $\sim 10^{-6}$.

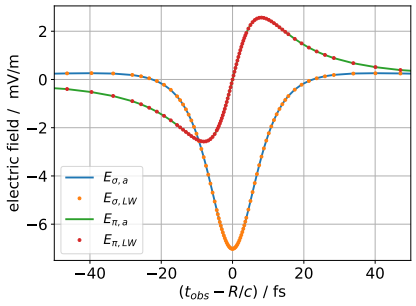

Figure 1: σ- and π-components of the electric field of a single electron in the time domain; curves show the analytic results, points are the results of our algorithm.

Figure 1 shows the two polarizations of the electric field of a single electron at a distance of 5 m. There is excellent agreement between the analytic result and our algorithm. The observer time covers the range between $(-2.6\,\mathrm{ps}, 2.8\,\mathrm{ps})$, but the peak only occurs in the narrow range ± 20 fs. Uniform sampling would require $\approx$ 2500 points, while only $\approx$ 100 non-uniformly spaced points are sufficient with adaptive sampling.

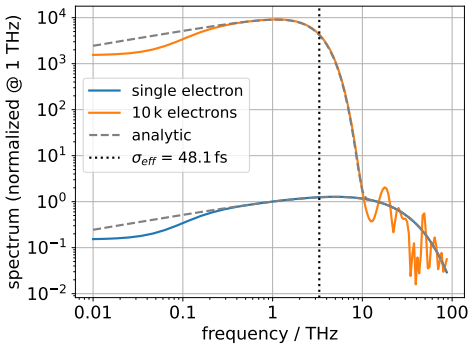

Figure 2: Radiation spectrum of 10 000 normally distributed electrons.

For the radiation spectrum, we consider 650 points on a screen, compute the electric field at each point in the time domain and then apply Eq. (4). One half of the points are on a regular grid, while the other are randomly distributed. The result for a single electron is shown as the blue curve in Fig. 2. Excellent agreement with the analytic result is obtained for frequencies greater than 400 GHz. The analytic result is obtained by integrating the spectrum over an infinite screen. However, smaller frequencies are emitted in 'cones' with larger opening angles. For frequencies in the range from 50 GHz to 400 GHz, part of the radiation vertically passes the screen and the intensity is reduced. Still, the radiation cone completely sweeps across the screen horizontally and the resulting spectrum is close to the analytic result both in spatial distribution and frequency dependence. For even smaller frequencies, corresponding to large times,

the radiation cone is so broad that it hits the screen at all times instead of sweeping across the screen. Effectively, the radiation appears on the screen instantaneously, which leads to spurious edge radiation (ER) with its characteristic flat spectrum.

We also consider a bunch of 10 000 electrons, with longitudinal positions drawn from a normal distribution of size $\sigma_l = 15\,\mu\text{m}$ ($\sigma_t = 50\,\text{fs}$). The computation takes about 5 min on an Apple M4 Max CPU with 48 GB of RAM. The orange curve in Figure 2 shows the coherent enhancement for frequencies smaller than $1/\sigma_t$, which agrees with Eq. (5). At larger, incoherent frequencies, the discrete sum over the random positions manifests itself as a random spectrum, that nonetheless follows the incoherent spectrum on average. By dividing the total spectrum by the incoherent spectrum, we can solve Eq. (5) for the form factor F and define the effective bunch length σ_{eff} as $F(1/\sigma_{\text{eff}}) = 1/e$. We find $\sigma_{\text{eff}} = 48.1\,\text{fs}$ close to σ_t.

SIMULATED BUNCH COMPRESSOR

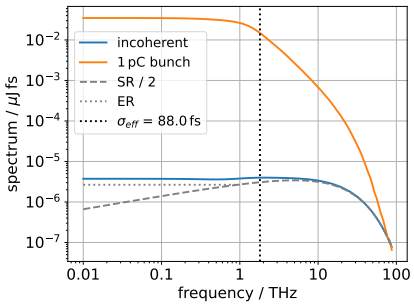

Figure 3: Integrated computed spectrum for a 1 pC bunch compressed from 380 fs to 3 fs. ER: edge radiation; SR: synchrotron radiation.

We simulated the bunch compression of a 1 pC electron bunch by a four dipole bunch compressor using `ASTRA` [8] with 10 000 macro-particles [9]. For the computation of the radiation, we only consider the path from before the last dipole, wherein the longitudinal bunch duration reduces from 380 fs to 3 fs. The observation screen is placed 230 mm downstream of the dipole. Due to the geometric setup, the radiation cones enter from the left.

The incoherent spectrum (blue curve in Fig. 3) is dominated by edge radiation up to 1 THz and synchrotron radiation for higher frequencies. The bunch reaches its few-fs bunch length only inside the fringe field of the exit edge, and the coherent radiation is dominated by edge radiation. Since the coherent radiation (orange curve in Fig. 3) also encodes the complex bunch evolution and radiation types, the effective bunch length is 88 fs.

Figures 4 and 5 show the spatial distribution on the screen at 100 GHz and 17.7 THz, respectively. At 100 GHz the typical 'doughnut' shape of edge radiation is clearly visible, which is in agreement with Fig. 3. Because radiation at this frequency is almost completely coherent, the shape does not depend on any sub-structure of the charge distribution. The

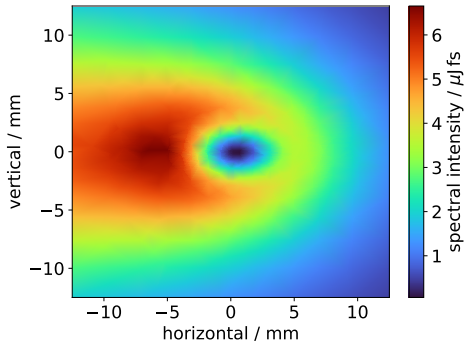

Figure 4: Computed spatial distribution of the spectral intensity at 100 GHz.

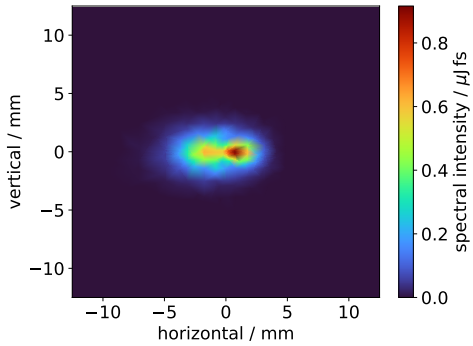

Figure 5: Computed spatial distribution of the spectral intensity at 17.7 THz.

horizontal bar of synchrotron radiation dominates the spectrum at 17.7 THz. Since this radiation is mainly incoherent, the 'granular' nature due to the macro-particle distribution is more pronounced.

CONCLUSION AND OUTLOOK

We present an algorithm to compute electromagnetic radiation by computing the Liénard-Wiechert fields in the time domain. To overcome the problem of solving the implicit equation for the retarded time in terms of the observation time, we instead solve for the observer time in terms of the retarded time. This allows to compute the coherent spectrum of 10 000 particles on arbitrary paths on a screen of 650 pixels in about 5 min. The results are in excellent agreement with analytical benchmarks.

As a next step, we plan to consider the Coulomb field as well. This will then serve as a starting point to compute transition radiation. To compute even more macro-particles, we want to build a surrogate model for the radiation fields.

REFERENCES

[1] J. D. Jackson, *Classical electrodynamics*. John Wiley & Sons, Inc., 1999.

[2] O. Chubar and P. Elleaume, "Accurate and Efficient Computation of Synchrotron Radiation in the Near Field Region", in *Proc. EPAC'98*, Stockholm, Sweden, pp. 1177–1179, Aug. 1998. `https://jacow.org/e98/papers/THP01G.pdf`

[3] T. Tanaka and H. Kitamura, "*SPECTRA*: a synchrotron radiation calculation code", *J. Synchrotron Radiat.*, vol. 8, no. 6, pp. 1221–1228, Nov. 2001. doi:10.1107/S090904950101425X

[4] R. D. Ryne, B. E. Carlsten, and N. A. Yampolsky, "Using a Lienard-Wiechert Solver to Study Coherent Synchrotron Radiation Effects", in *Proc. FEL'13*, New York, NY, USA, Aug. 2013, pp. 17–23, 2013. https://jacow.org/FEL2013/papers/MOOCNO04.pdf

[5] A.-S. Müller and M. Schwarz, "Accelerator-based THz radiation sources", in *Synchrotron Light Sources and Free-Electron Lasers: Accelerator Physics, Instrumentation and Science Applications*, E. J. Jaeschke, S. Khan, J. R. Schneider, and J. B. Hastings, Eds. Cham: Springer International Publishing, 2020, pp. 83–117. doi:10.1007/978-3-030-23201-6_6

[6] B. Nijholt, J. Weston, J. Hoofwijk, and A. Akhmerov, "*Adaptive*: parallel active learning of mathematical functions", 2019, doi:10.5281/zenodo.1182437,

[7] M. Schwarz, P. Basler, M. v. Borstel, and A.-S. Müller, "Analytic calculation of the electric field of a coherent THz pulse", *Phys. Rev. Spec. Top. Accel. Beams*, vol. 17, no. 5, p. 050701, May 2014. doi:10.1103/PhysRevSTAB.17.050701

[8] K. Flöttman, "A space charge tracking algorithm", https://www.desy.de/~mpyflo/,

[9] M. Yan, A.-S. Müller, M. J. Nasse, M. Schuh, and M. Schwarz, "Optimization of THz Radiation Pulses at FLUTE", in *Proc. IPAC'16*, Busan, Korea, pp. 3067–3069, Jun. 2016. doi:10.18429/JACoW-IPAC2016-WEPOY037